Correlation Between Molecular Structure, Free Volume, and Physical Properties of a Wide Range of Main Chain Thermotropic Liquid Crystalline Polymers

TSUNG-TANG HSIEH,[1] CARLOS TIU,[2] GEORGE P. SIMON[3]

[1] UMC, Advanced Technology Development, Hsin-Chu, Taiwan 30077

[2] Department of Chemical Engineering, Monash University, Clayton, Victoria, Australia 3168

[3] Department of Materials Engineering, Monash University, Clayton, Victoria, Australia 3168

Received 16 November 2000; accepted 27 January 2001

ABSTRACT: Physical phenomena such as glass transition temperatures, melting points, and relaxational behavior have been determined for a wide range of thermotropic liquid crystalline polymers (TLCPs) and polycarbonate (PC). Damping intensities of rigid TLCPs during glass transition are greater than those of semirigid and semiflexible TLCPs. Positron annihilation lifetime spectroscopy was also employed to evaluate free volume parameters of polymers. In general, the positron annihilation lifetime spectroscopy (PALS) free volume parameters show that all TLCPs have much smaller, fewer free volume sites compared with PC. Correlations were found between PALS free volume parameters and glass transition temperature, dynamic mechanical damping strength, and bulk density where greater free volume parameters corresponded to higher glass transition temperatures, greater damping strength, and lower density.
 J Appl Polym Sci 82: 2252–2267, 2001

Key words: thermotropic liquid crystalline polymer; glass transition; positron annihilation; free volume

INTRODUCTION

Main chain thermotropic liquid crystalline polymers (TLCPs) have been extensively studied in recent times, particularly in relation to their mechanical properties and rheology. The chain rigidity and high degree of alignment possible in TLCPs often result in a high modulus (especially if measured in the direction of molecular alignment). Such a rigid chain conformation with its lack of entanglements leads to low melt viscosity, small or negative die swell, and long relaxation times.[1] Most commercially available TLCPs or those that have been under development with industrial applications in mind are polyesters with two or three constituent monomers. While the effect of molecular structure on the physical properties (such as thermal and relaxational behavior and orientation) have been widely studied,[2–5] far less has been reported on the microscopic packing of these materials and the manner in which this relates to a macroscopic property such as density. This is of fundamental interest since it involves rheology and mechanical properties. Furthermore, it is the packing of TLCPs that gives them their thermally processable nature. If LCPs are too perfectly packed and strongly asso-

Correspondence to: George P. Simon (george.simon@spme.monash.edu.au).

Journal of Applied Polymer Science, Vol. 82, 2252–2267 (2001)

ciating, they may behave like the well-known lyotropic aromatic polyamide fiber (Kevlar) processable only from solution. The two primary strategies to ensure a reduction in crystalline melting temperature and a low viscosity to allow TLCPs to be processed by conventional plastic processing equipment are the incorporation of (a) flexible units and (b) rigid units that are able to reduce the linearity of the chain.[6] This is emphasized later in this paper where examples of such materials are given.

This work includes evaluating the excluded or free volume by a subatomic, nondestructive probe technique known as positron annihilation lifetime spectroscopy (PALS). The scientific basis of this technique is presented shortly where its applicability as a potent measure of the microscopic space between chains on an ångstrom scale is indicated. A wide range of polymers, mainly TLCPs, has been chosen in this study. In addition to free volume behavior evaluated by PALS, the relaxational properties of these materials will also be investigated. This is done to allow simple structure–property relationships to be obtained and to correlate such properties with the free volume sampled by PALS.

Background to PALS

A positron is the antiparticle of an electron and has almost the same physical properties as an electron but bears an opposite (positive) charge. If a collision takes place between an electron and a positron, the two will annihilate with each other and create a burst of energy. Although a positron can exist for infinite time in a true vacuum environment, the positron will be annihilated if surrounded with condensed materials through one of three mechanisms. Each positron annihilation mode has its own characteristic lifetime (the time between its birth and annihilation with an electron). The fastest annihilation mechanism is the formation of the hydrogen-like atom, *para*-positronium (*p*-Ps), which consists of an electron and a positron in the antiparallel spin state. *p*-Ps has a lifetime of 0.125 ns and its annihilation gives two γ-rays. The second fastest annihilation occurs when a free positron directly collides with an electron leading to emission of 1–3 photons. The longest lifetime of the positron annihilation is through the formation of an *ortho*-positronium (*o*-Ps), a bound pair of a positron and an electron in the parallel spin state. In vacuum, the annihilation of an isolated *o*-Ps has a characteristic lifetime of 140 ns, producing three γ-rays. By contrast, in condensed media, *o*-Ps can exist no longer than 9 ns due to the pick-off or quenching process in which the *o*-Ps annihilates by picking off an orbital electron with opposite spin from neighboring molecules, and thus it produces two γ-rays, instead of three.

It is the last mode of positron annihilation that is of most importance in material research because the *o*-Ps annihilation via the pick-off mechanism occurs predominantly in the region where electron density is low. Vacancy-type defects in metals and ceramics and free volume sites in polymers are the locations where such pick-off process takes place as *o*-Ps is pushed toward them due to repulsion by positive charged atomic nuclei of the surrounding molecules.[7,8]

If the positrons annihilate in a material with a perfect crystalline structure, they will all experience the same environment and thus display only one mode of annihilation. Therefore, the lifetime distribution of the positrons in such matters is a simple exponential decay curve,[9]

$$N(t) = \exp(-\xi t) \tag{1}$$

where $N(t)$ is the fraction of the positron remaining at time t, and ξ represents the rate of positron annihilation.

For semicrystalline or amorphous materials, positrons will encounter various molecular environments such as free volume sites and crystalline defects. A positron lifetime spectrum can be expressed as a sum of exponentially decaying lifetime components,

$$N(t) = \Sigma_i I_i \exp(-\xi_i t) \tag{2}$$

where I_i and ξ_i represent the intensity of the positron and the positron annihilation rate, respectively, by the ith mode. The lifetime of the positron at the ith mode can be obtained from the reciprocal of ξ_i ($\tau_i = 1/\xi_i$). It is usually found that a spectrum of a polymeric material can be fitted with three mean lifetimes, corresponding to the annihilation of *p*-Ps (τ_1, I_1), free positron (τ_2, I_2), and *o*-Ps (τ_3, I_3). The mathematical expression of this three-mode decay curve is

$$N(t) = I_1 \exp(-t/\tau_1) + I_2 \exp(-t/\tau_2) + I_3 \exp(-t/\tau_3) + \Delta \tag{3}$$

where Δ is the value of the background decay. From this equation, I_1, I_2, and I_3 can be obtained as the zero time intercepts and τ_1, τ_2, and τ_3 as the reciprocals of the slopes, by fitting the decay curve with three straight lines, corresponding to three modes of annihilation. Values of the longest lifetime parameters (τ_3 and I_3) have been found to be closely related to free volume. A larger free volume site leads to a longer τ_3, and a higher number concentration of free volume sites lead to a greater value of I_3.

The magnitude of the free volume radius can be estimated using the following semiempirical equation[10] by assuming τ_3 is 0.5 ns in the case of an environment without free volume; the size of the free volume site can be approximated by a spherical potential well with radius R,

$$\tau_3 = \frac{1}{2}\left[1 - \frac{R}{R_0} + \frac{1}{2\pi}\sin\left(\frac{2\pi R}{R_0}\right)\right]^{-1} \quad (4)$$

where τ_3 is the *o*-Ps lifetime. $R_0 = R + \Delta R$ where ΔR is the fitted empirical electron layer (and equals 1.66 Å) from molecular crystals with known vacancy sizes. As τ_3 generally ranges from 0.5 to 3 ns, the mean radius of free volume sites in polymers is approximately from 1 to 6 Å.

The average volume of free volume sites V_f, assuming a spherical geometry, can then be calculated as

$$V_f = \frac{4}{3}\pi R^3 \quad (5)$$

The total free volume fraction h_f expressed in percentage, can be determined from the equation[11]

$$h_f = CV_fI_3 \quad (6)$$

where C is a constant empirically determined from comparison with pressure–volume–temperature (PVT) data. For common glassy polymers, C has been found to range[7] from 1×10^{-3} to 2×10^{-3}. For examples, epoxy[11] has a C value of 1.8×10^{-3} and PS has a C value[12] of 1.4×10^{-3}. A somewhat large value of C, 6.5×10^{-3}, was reported for poly(chlorotrifluoroethylene) (PCTFE),[13] which could result from the inhibition of *o*-Ps formation by its halogen moieties.[14]

Brandt et al.[15] examined the pick-off process in different lattices and concluded that the free volume sites are the main locations where the pick-off annihilation of *o*-Ps takes place. The validation of the application of PALS on the determination of free volume properties has been quantitatively verified in some cases. Kobayashi et al.[16] found a good correlation between τ_3 and free volume estimated from the group contribution method for various polymers. The fractional free volume distribution of a glassy polystyrene was found to agree well between data obtained from PALS and the free volume theory by Simha and Somcynsky.[12] Schmidt and Maurer[17,18] reported a good agreement between the free volume parameters calculated from PALS and PVT on the blends of poly(ethylene oxide) (PEO) and poly(methyl methacrylate) (PMMA). Some factors, such as temperature,[19] pressure,[20] and degree of crystallinity,[21] influence the PALS parameters the same way as they would affect free volume.

EXPERIMENTAL

Materials

A selection of seven TLCPs and a flexible engineering polymer whose chemical structures are shown in Figure 1 were used in this study. These TLCPs were chosen specifically to include semicrystalline and amorphous, fully aromatic and aliphatic-aromatic polymers, as well as materials with different degree of flexibility. They are all general-purpose, unfilled grades and supplied in pellet form. The engineering thermoplastic chosen for comparison with TLCPs was bisphenol-A type polycarbonate, which is a conventional, flexible-chain amorphous thermoplastic despite its high degree content of aromatic units.

Vectra TLCPs are members of wholly aromatic, semicrystalline copolyesters or polyester-amides obtained from Ticona (USA) (formerly Hoechst-Celanese). Vectra A950 (referred to as Vectra-A hereafter) is a well-studied TLCP that consists of 73 mol % *p*-hydroxybenzoic acid (HBA) and 27 mol % 2-hydroxy-6-naphthoic acid (HNA), as shown in Figure 1(a). VectracC950 (referred to as Vectra-C) is also based on HBA and HNA [Fig. 1(b)], and its precise composition has not been revealed. Based on the correlation between melting points of HNA/HBA polymer and their HNA contents,[22] Vectra-C with a melting point of 327°C indicated by the product data sheet may contain either higher concentrations of HNA or HBA than Vectra-A. It is favorable to manufacture HNA/HBA TLCPs with high HBA content

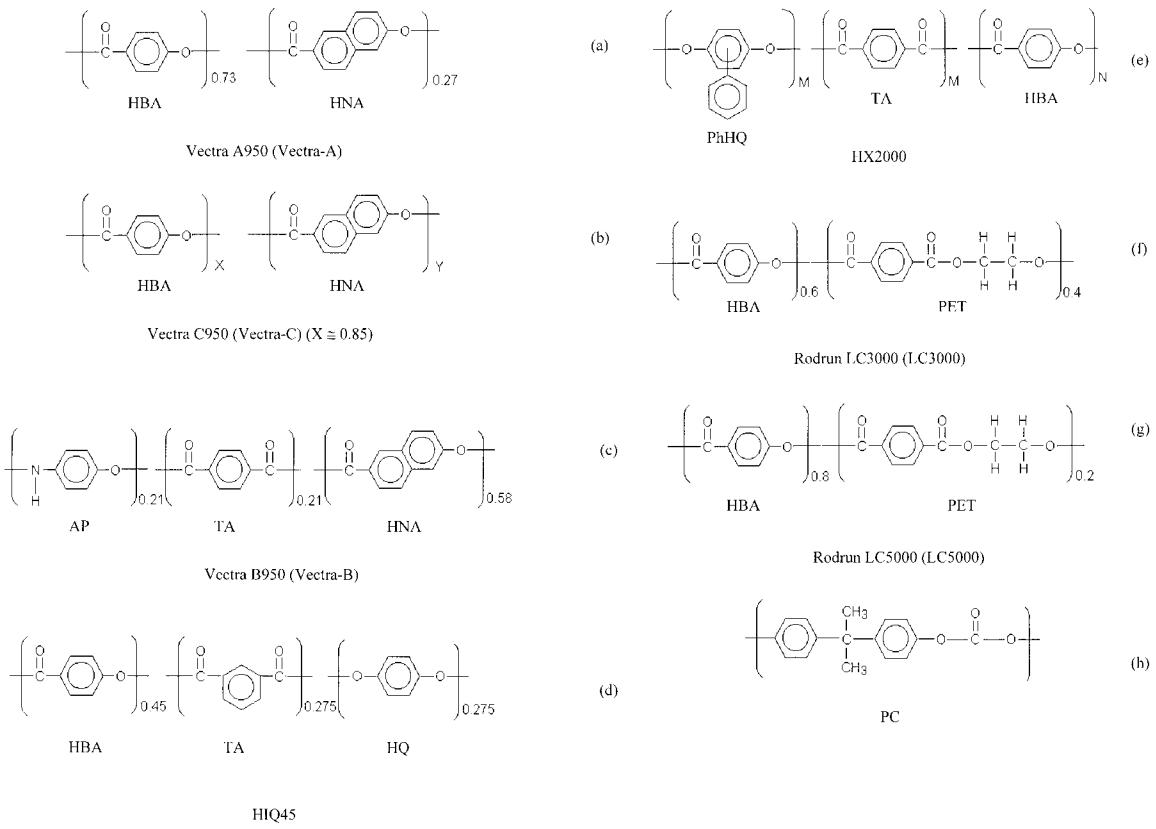

Figure 1 Chemical structures of TLCPs and PC used in this study.

because HNA is generally the most expensive monomer to produce in such copolyesters, although T_ms of such TLCPs are expected to be higher. The molecular weights of these (and other) TLCPs can not be measured by gel permeation chromatography (GPC), as they do not readily dissolve in appropriate solvents. The weight-average molecular weight (M_w) of Vectra-A is about 30,000, a value derived from its intrinsic viscosity,[23] and represents one of the few reported values among the commercial TLCPs.

Unlike Vectra-A and Vectra-C, which belong to the polyester family, Vectra B950 (labeled as Vectra-B) is a terpolymer and polyesteramide that consists of 600molb% HNA, 20 mol % terephthalic acid (TA) and 20 mol % aminophenol (AP). Its molecular structure is shown in Fig.1(c).

HIQ45 is a semicommercial TLCP obtained from the research laboratory of Ticona. Its terpolyester structure can be seen in Fig.1(d) and it comprises 45 mol % HBA, 27.5 mol % isophthalic acid (IA) and 27.5 mol % hydroquinone (HQ). Incorporation of a disruptive comonomer is commonly used to reduce the melting point of TLCPs. In the case of Vectra materials the 2,6-linked naphthalene unit is introduced to encourage a loss of chain linearity. Similarly, meta-linked aromatic rings (isophthalene units) are incorporated as part of HIQ45. TLCPs such as HIQ45 are favored because they do not contain the expensive HNA monomers.

HX2000 belongs to a class of materials, HX series, manufactured at various times by DuPont that vary in crystallinity from semicrystalline (e.g., HX4000, HX6000, HX8000) to amorphous (HX1000, HX2000). The HX series are believed to be wholly aromatic TLCPs with bulky side groups. HX4000 has been reported to contain TA, HQ, and phenyl hydroquinone (PHQ).[24] HX2000 is the only amorphous TLCP used in this research. Detectable crystallinity of HX2000 has been shown to be possible only after prolonged and careful heat treatment.[25] Such heat treatment was not been applied in this work and any possible annealing effect has been avoided to preserve its amorphous features. The molecular structure is likely to be a terpolyester composing of TA, PHQ, and possibly a very small amount of HBA[6] as demonstrated in Fig.1(e). Precise con-

centrations of the constituents of HX2000 are not known.

Rodrun TLCPs are based on HBA and poly(ethylene terephthalate) (PET) and obtained from Unitika, which is licensed to produce these materials from Eastman Chemicals. The PET/HBA TLCP was originally manufactured by (then named) Tennessee Eastman under the name X7G. Rodrun LC3000 (referred to as LC3000 hereafter) consists of 60 mol % HBA and 40 mol % PET, while Rodrun LC5000 (referred to as LC5000 hereafter) consists of 80 mol % HBA and 20 mol % PET, as seen in Figure 1(f) and Figure 1(g), respectively. The molecular weight of the Eastman PET/60PHB TLCPs has been reported to be around 20,000 using the intrinsic viscosity method.[26,27]

TLCPs whose rigidity is reduced without the introduction of flexible spacers are called "semirigid" TLCPs, while the term "semiflexible" is used for TLCPs with flexible spacers.[6] Despite no clear boundary between rigid and semirigid TLCPs, TLCPs such as Vectra materials are regarded as rigid TLCPs and TLCPs with structure shown in Figure1(d) are considered semirigid TLCPs in this work. TLCPs such as Rodrun materials are referred to as semiflexible TLCPs due to their ethylene moieties.

A bisphenol-A type polycarbonate (referred to as PC hereafter) whose molecular architecture is shown in Figure 1(h) was also used. It serves as a model thermoplastic for the purpose of comparison with TLCPs. The PC is Lexan 134, obtained from GE Plastics, Australia. Based on GPC, the weight- (M_w) and number-average molecular weight (M_n) are 69,000 and 36,000, respectively.

All polymers were dried at 100°C in a vacuum oven for 24 h. Compression-molded platens of 20mm thickness were prepared by a laboratory pneumatic press under a pressure of 200MPa for 5 min. The platens were then quenched to room temperature quickly by removing the mold assembly to another press cooled by a running water jacket.

Experimental Techniques

A DuPont 9900 thermal analyzer with a differential scanning calorimetry (DSC) module was used to study the thermodynamic transitions of the materials. All samples of 10–15 mg were initially scanned over a temperature range from 50°C to the final temperature at a heating rate of 20°C/min and cooled to 50°C at a cooling rate of 20°C/min immediately upon attaining the final temperature. All samples were then scanned again from 50°C to the final temperature at the same heating rate. The measurements were carried out with a continuous nitrogen gas flow of 60 cm^3/min. The reported results were taken from the second heating runs of the experiments to avoid the experimental artifacts arising from previous thermal history. The temperature of the instrument was calibrated using indium and zinc standards.

DMTA was undertaken using the Perkin Elmer DMA-7 (DMA-7) and the Rheometrics dynamic analyzer II (RDAII). The three-point-bend mode was employed for samples tested by DMA-7 at a frequency of 1 Hz and a scan rate of 2°C/min with a continuous helium gas flow of 40 cm^3/min. The sample dimension was 20 × 5 × 2 mm. The RDAII was equipped with rectangular torsion fixtures for oscillatory shear deformation test on solid samples. In order to compensate for thermal expansion of the sample during torsion testing, the auto tension function was enabled, which automatically maintained a 10 N tension force on the sample. Specimen dimensions were 50 × 5 × 2 mm. They were oscillated at 1 Hz in a 2°C step with a soak time of 11minute to obtain thermal equilibrium.

The PALS measurements were made on an automated EG&G Ortec fast–fast coincidence system using a ^{22}Na spot source of approximately 2 mm in diameter and instrument resolution of 270 ps. The equipment was thermally equilibrated in an air-conditioned laboratory maintained at 22 ± 1°C to avoid electronic drift. The source of 1.3 MBq was contained between two 2.5 μm thick titanium foils. No considerable source contribution due to the titanium foils was found based on measurements of 99.99% pure, annealed, and chemically polished aluminum samples that show a single lifetime spectrum of 166 ps. The source-sample assembly was made by sandwiching the source between two pieces of polymer coupons of 20 × 20 × 2 mm. At least 10 spectra were obtained each with 30,000 peak counts (roughly 1 million overall counts) and were analyzed using the PFPOSFIT program with a three-parameter model. In order to numerically fit the PALS spectra, the shortest lifetime was set at 0.125 ns which is the characteristic lifetime of *p*-Ps annihilation in molecular solid.

Due to the strength of the radioactive isotope decaying with time, PALS measurements were conducted within a given time. The positron source, ^{22}Na, used in this work has been shown

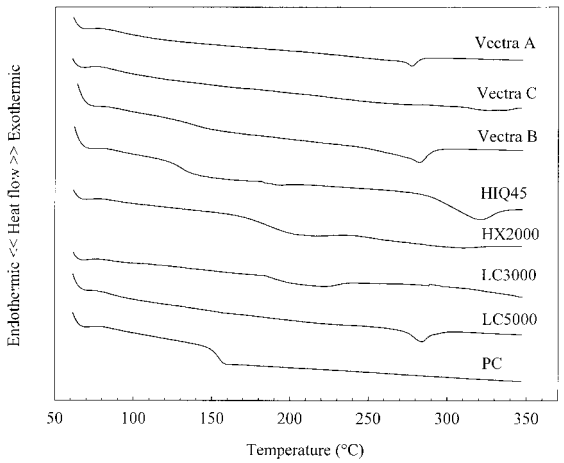

Figure 2 DSC thermograms of TLCPs and PC at 20°C/min.

able to last for 200 days of use before any serious reduction of source strength. The values of τ_3 and I_3 measured on PC at times elapsed from the new ^{22}Na source showed a less than 2% variation in 200 days.[28] The reported PALS data in this work were collected in 100 days following the preparation of the source.

Solid densities of the materials were measured by using a Micromeritics Accupyc 1330 gas displacement pycnometer. It determines the volume and density of the test sample by measuring the pressure change of helium in a calibrated volume. The sample weight was obtained from a four-digit electrical microbalance and keyed into the pycnometer to calculate the density. The as-molded samples were purged by helium ten times to ensure a consistent, dry atmosphere on testing. The mean density of the sample was obtained from ten measurements at ambient temperature under a helium atmosphere.

RESULTS AND DISCUSSION

Most thermal properties and dynamic mechanical thermal properties of the TLCPs used in this study can be found in the literature for various experimental conditions. Properties of TLCPs have been known to susceptible to the thermal and/or mechanical history they experience before testing. Therefore, it is necessary to carry out all measurements on samples processed in the same way and using the same test conditions, as previously described in the experimental section.

Thermal Properties

Figure 2 shows the thermograms of various TLCPs and PC measured by DSC and the thermal transitions of the materials are summarized in Table I.The reported T_m values are peak temperatures and the T_g values are determined by the midpoint method.[29] Except for HIQ45 and HX2000, TLCPs show weak and ill-defined glass transition behavior in their DSC thermograms. TLCPs like Vectra polymers do not show distinct slope changes in the DSC thermograms when compared with that of a flexible polymer, PC. Although the thermograms of HIQ45 and HX2000 do display clear slope changes, their glass transitions are much less apparent than flexible polymers such as PC. Instead of becoming rubbery, the so-called glass transition experienced by TLCPs seems to increase the molecular mobility to an extent much less than for flexible polymers.

Both HIQ45 and HX2000 are terpolymers, consisting of three different ester units, rather than the two in Vectra-A and Vectra-C. This could result in a greater diversity of molecular environments in them, possibly frustrating tight packing. In addition, the meta-linkages in HIQ45 molecules make them less straight (lower persistence length), and the bulky phenyl substituents of HX2000 also hinder close packing. As a result, they behave somewhat more TP-like and show prominent glass transition behavior compared with the other TLCPs studied.

The melting behavior is also different between samples. TLCP melts still maintain a degree of molecular order following melting because of the liquid crystalline state, and thus the heats of fusion (ΔH_f) of TLCPs (if any) are small compared with those of crystalline flexible polymers in the

Table I Thermal Transitions of TLCPs and PC Measured by DSC

Materials	T_g (°C)	T_m (°C)	ΔH_f (J/g)
Vectra-A	—[a]	278	0.92
Vectra-C	—[a]	325	1.23
Vectra-B	—[a]	282	2.69
HIQ45	130	317	5.69
HX2000	184	—[b]	—[b]
LC3000	—[a]	218	3.78
LC5000	—[a]	283	1.72
PC	152	—[b]	—[b]

[a]Too weak to be determined by DSC.
[b]Melting phenomena not observed.

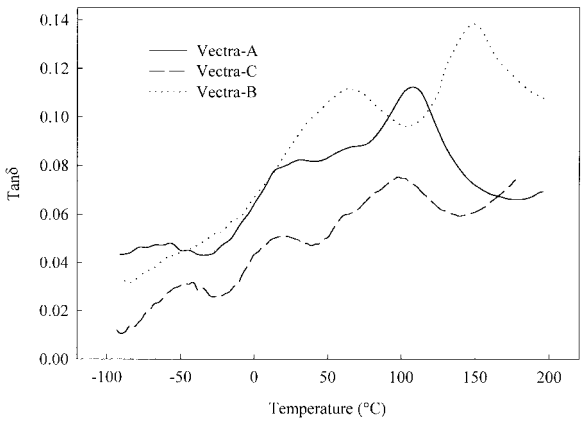

Figure 3 The tanδ spectra of Vectra-A, Vectra-C, and Vectra-B using DMA-7 at 1 Hz.

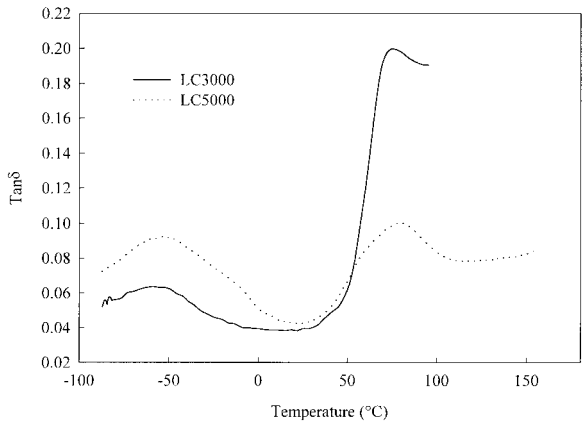

Figure 4 The tanδ spectra of LC3000 and LC5000 using DMA-7 at 1 Hz.

literature. Vectra-A and Vectra-C have ΔH_f values only about 1 J/g. The greater ΔH_f found from Vectra-B is probably due to the presence of amide groups that are capable of forming strong hydrogen bonds, and thus there is a higher enthalpic change involved in disrupting these bonds. HIQ45 has been reported to be biphasic in the molten state.[30,31] In the sense that it is able to pass into the isotropic melt state at a temperature before degradation occurs, it demonstrates the largest ΔH_f among the TLCPs studied. This is presumably because some crystallites melt into the isotropic phase, where greater enthalpic differences exist between ordered crystalline phase and disordered isotropic phase. HX polymers can be either amorphous or semicrystalline,[24,32] most likely depending on the concentration of the phenyl substituents. In the case of HX2000, it appears to be an amorphous TLCP, as originally claimed by the manufacturer and thus no melting peak is observed.

For Rodrun polymers, the T_m of the TLCP increases from 218 to 283°C and the ΔH_f decreases from 3.78 to 1.72 J/g when the HBA content increases from 60 mol % (LC3000) to 80 mol % (LC5000). This indicates that the observed melting behavior results from the melting of the PET-rich phase in the Rodrun TLCPs, because the T_m of PET is around 240°C [33] and the similar PET/PHB TLCPs manufactured by Tennessee Eastman have been shown to be compositionally heterogeneous in nature.[2,34] In addition, the T_m of the homopolymer of HBA is claimed to be as high as 445°C.[35] It has been shown that the T_m of the PET-rich phase in the PET/PHB TLCPs reduces with increasing HBA content up to 60 mol % due to the early nucleation or a dilution effect induced by the incorporation of HBA moiety.[2] The ΔH_f values of the PET-rich phase in the Rodrun TLCPs are generally between about 2– J/g and decrease with the incorporation of HBA.[2,36] Note that the value of ΔH_f strongly depends on the thermal history, and heat treatment such as annealing has a significant effect on both T_m and ΔH_f.[2] The influence of thermal history is beyond the scope of this work.

Dynamic Mechanical Properties

The tanδ curves of the TLCPs and PC using the Perkin-Elmer DMA-7 in the three-point bending mode at 1 Hz with a heating rate of 2°C/min are shown in Figures 3–5.

There are three molecular relaxation processes observed, the peak temperatures of two major

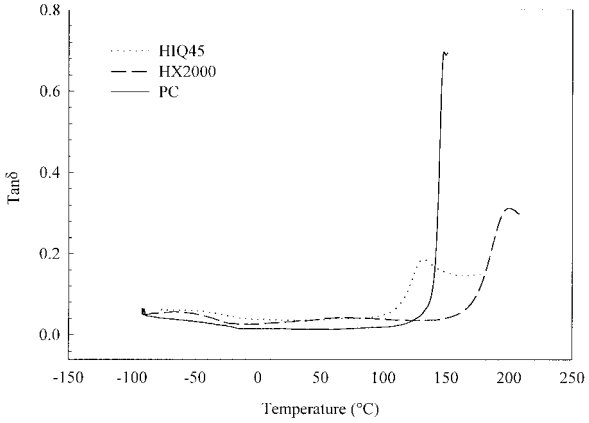

Figure 5 The tanδ spectra of HIQ45, HX2000 and PC using DMA-7 at 1 Hz.

relaxations at about 100 and 30°C and a weak relaxation at about −50°C, in the tanδ curve of Vectra-A, as seen in Figure 3. According to the nomenclature used for flexible polymers, they will be named α-, β-, and γ-relaxations in the order of decreasing peak temperature. The weak γ-relaxation is attributed to the motion of phenylene units in HBA.[4,5,37] Because this relaxation is a very localized motion involving only a small portion of the main chain, the relaxation temperature is independent of the composition of the HNA/HBA TLCPs.[38] The β-relaxation was shown to result from the local reorientation of the HNA moieties.[39] The α-relaxation temperature or T_g is associated with the onset of the cooperative micro-Brownian motion along the main chain found in flexible polymers.[40] Because Vectra-C contains the same kinds of monomers as Vectra-A, all three relaxations shown by Vectra-A can also be found in the tanδ curve of Vectra-C, as also shown in Figure 3. Although its detailed chemical compositions have not been released by the supplier, the HNA content of Vectra-C has been estimated to be around 15 mol % by using dielectric relaxation method.[41]

Vectra-B also shows three relaxations, as also shown in Figure 3, because it possesses similar moieties as Vectra-A and Vectra-C (Fig. 1). Vectra-B shows the highest T_g among Vectra TLCPs due to its amide groups that form strong hydrogen bonds and limit chain mobility. It has been reported that the existence of amide links in an ester environment can effectively increase T_g of the TLCPs.[42] A high T_g is an important requirement for polymers used as structural materials at elevated temperatures since the mechanical performance of the polymers usually decreases sharply when the glass transition occurs. The β-relaxation of Vectra-B is both greater in the relaxation temperature and intensity because it consists of more HNA (60 mol %) compared with that of Vectra-A (27 mol %) and Vectra-C (ca. 15 mol %). While the temperature location of the relaxation relating to HBA is independent of composition, the relaxation relating to HNA moiety has been found to depend on concentration.[38] Also observed in Fig. 3, is a shoulder peak in both tanδ curves of Vectra-A and Vectra-C between their α-and β-relaxations. This could arise from the molecular relaxations involving particular sequences or combinations of HNA-rich segments.

Figure 4 shows the tanδ curves of LC3000 and LC5000 by DMA-7. There are only two relaxations observed in the tanδ curves of Rodrun materials, as they do not contain naphthalene units. The α-relaxation observed at around 80°C has been assigned to the glass transition of the PET-rich phase.[43] The α-relaxation of the HBA-rich phase has been reported to occur between 160 and 190°C,[43,44] although it is not often observed. The Rodrun samples studied here were fractured by the action of the probe of the DMA-7 at temperatures greater than 150°C despite the small force of about 900 mN used. No α-relaxation relating to the HBA-rich phase was thus able to be detected. As discussed previously, LC order appears to restrain the intensity of α-relaxation of TLCPs. LC5000 has the intensity of α-relaxation similar to Vectra TLCPs (close to that of Vectra-A and Vectra-C, but still lower than Vectra-B) as seen in Table II, while LC3000 displays a greater tanδ intensity than LC5000 due to its higher PET content. With reference to the T_g of pure PET (78°C),[2] the increase of HBA concentration seems to have little effect on T_g values as T_g of LC3000 and LC5000 are 75 and 83°C, respectively. This indicates a limited miscibility of HBA in the PET-rich phase. The secondary relaxation of the Rodrun TLCPs is also due to the rotation of phenylene rings, also the cause of the relaxations of Vectra TLCPs. Compared with Figure 3, the change of chemical environment due to different comonomers of the TLCPs does not affect the temperature of this secondary relaxation much. With a greater HBA concentration, the intensity of secondary relaxation of LC5000 is stronger than that of LC3000, and even becomes comparable to its α-relaxation.

Due to their much stronger damping behavior compared with those TLCPs in Figures 3 and 4, tanδ curves of HIQ45, HX2000, and PC are plotted together in Figure 5. The greater damping behavior of HIQ45 apparently results from its IA moiety, which interrupts the otherwise all-*para* chain linearity. The kinked links, such as IA moiety, have been reported to be an effective way to reduce T_m and increase the T_g of TLCPs.[42] It is clear that the steric effect, arising from the phenyl pendant along the all-*para* aromatic molecular chains, predominantly affects the HX2000 chain packing. The bulky substituents of the HX2000 serve to keep the HX2000 chains somewhat apart and even distort the chain linearity due to the orientation of the substituents.[42] Therefore, the highest T_g value, and also the greatest damping intensity, occur for HX2000 amongst all the TLCPs studied.

Table II Comparison of T_g and Intensity of tan δ Peak Measured by DMA-7 and RDAII at 1 Hz

Materials	T_g (°C) (DMA-7)	tan δ (DMA-7)	T_g (°C) (RDAII)	tan δ (RDAII)
Vectra-A	100	0.11	98	0.07
Vectra-C	99	0.08	96	0.07
Vectra-B	146	0.14	136	0.11
HIQ45	132	0.19	123	0.20
HX2000	200	0.31	185	0.40
LC3000	75	0.2	59	0.19
LC5000	81	0.1	73	0.06
PC	154	0.87	153	1.59

The aromaticity of PC is similar to LC3000 (Fig.1) but shows significantly stronger damping behavior. This is because, in addition to the methyl substituents that frustrate packing, its rigidity is significantly reduced due to the presence of carbonate linkages which are flexible and rotate easily. This clearly illustrates the dissimilar damping nature of TLCPs and flexible polymers. Since the glass transition phenomena of amorphous polymers result from free volume sites created by the long, flexible chains that entangle with each other in the amorphous bulk, it is understandable that rigid TLCPs show a lesser degree of damping behavior in the glass transition. It has been proposed that the α-relaxations of the TLCPs might only transform the materials from a glassy state to a mobile nematic state, instead of the rubbery state displayed by flexible polymers.[4] In fact, after passing through the glass transition temperature, the TLCPs studied still remain "glass-like" according to the observation of the DMA-7 probe displacement. For example, there was no mark left by the oscillating probe on the surface of the TLCP sample after completion of the test (30–50°C above T_g). Conversely, the PC sample had a distinct mark created by the probe due to permanent deformation following the glass transition region.

Note that glass transitions of TLCPs have been found to closely depend on their molecular order induced by varying chemical structures or applying thermal treatment (annealing).[3,45] Smectic polyesters have been shown to have lower T_gs compared with that of isotropic polyesters with similar chemical structures, while temperature of γ-relaxation is higher for smectic samples than for isotropic ones.[45] This was attributed to the more stretched conformation of the flexible spacers in the smectic structure.[45] It has been reported that annealed TLCPs showed increase in T_g due to the development of molecular order that leads to constraint of molecular mobility.[3] In this work, samples were quenched to room temperature after platen press at above T_m completed. This procedure can erase previous thermal history and avoid any annealing effect so that the discussion of the properties of TLCPs can be limited on molecular structures achieved under these processing conditions.

Table II lists values of T_g and tanδ from DMA-7 and RDAII. Because the effective heating rate of RDAII, including isothermal soak and measurement time, is lower than that of DMA-7, values of the glass transition of materials measured by RDAII are all lower than those obtained by DMA-7. The intensities of the glass transitions of the polymers determined by RDAII show a similar trend to those measured by DMA-7. Vectra TLCPs and LC5000 have low tanδ intensities of the α-relaxations, whilst PC, HIQ45, HX2000, and LC3000 display high tan intensities.

In general, the storage modulus of a flexible polymer maintains a constant value at low temperatures in the glassy state, decreasing sharply at the point when glass transition occurs. This is clear from the shear storage modulus curve of PC measured by RDAII at 1 Hz in Figure 6. The onset of glass transition seriously decreases its mechanical performance as the polymer chains become mobile. By contrast, the shear storage modulus G' of the rigid TLCP such as Vectra-A begins decreasing at temperatures well below its T_g and no sharp decrease at the glass transition region is observed, although the α-relaxation is indeed observed as a maximum in its tanδ curve (Fig. 3). This is due to the close-packing and low entanglement density of rigid TLCP molecules compared with flexible thermoplastics. Without entangle-

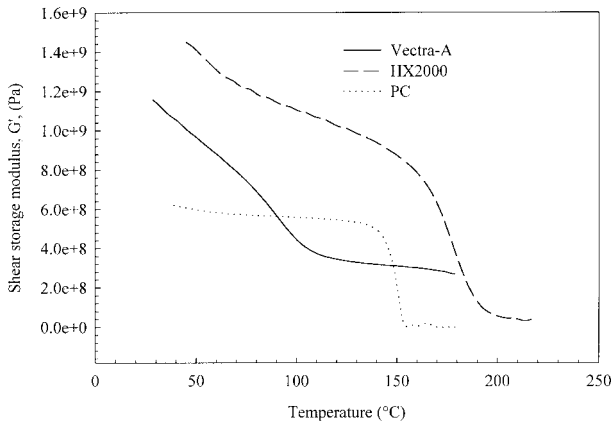

Figure 6 Shear storage moduli of Vectra-A, HX2000, and PC using RDAII at 1 Hz.

ments to function as physical crosslinks and thus hinder chain motion, slippage between adjacent chains is more likely to occur in TLCPs. Therefore, molecular relaxation processes take place gradually in response to an applied deformation as a function of increasing temperature, rather than more collectively as for the glass transition of PC. This is also related to the fact that the β-relaxation of Vectra-A is very close in nature and coupled to the α-relaxation, as seen by their similar intensities in Figure 3. As discussed previously, α-relaxations of rigid chain polymers are essentially a limited motion of the main chain, which can be seen by the low magnitude of the α-relaxations. Therefore, at temperatures for which phenylene units (γ-relaxation) and naphthalene units (β-relaxation) have been relaxed in a local fashion, there are only limited chain motions remaining and able to take place at the α-relaxation.

The behavior of G' of HX2000, the amorphous TLCP, is somewhat intermediate between that of PC and Vectra-A. Instead of maintaining a constant modulus at low temperatures as does PC, G' of HX2000 decreases slowly with temperature like Vectra-A. However, a rather noticeable decrease in its storage modulus occurs at the glass transition region. The LC nature of HX2000 appears to allow molecular relaxation to a similar extent as Vectra-A prior to its glass transition. The bulky substituents along the HX2000 main chain reduce the perfection of molecular packing and thus the coordination of chain movement for interchain slippage. The lack of crystallinity in HX2000 may also contribute to its similarity in behavior in this respect to PC (i.e., dramatic decrease in G'), which is also an amorphous polymer, compared with other semicrystalline TLCPs. In addition, both Vectra-A and HX2000 exhibit greater values of G' than PC at low temperatures, retaining higher values of G' at temperatures above glass transition as well.

Free Volume Behavior

The mean value of *o*-Ps lifetime, τ_3, is indicative of the mean size of free volume sites in polymeric materials. Table III details the PALS parameters, derived physical quantities and densities of the polymers. The τ_3 values obtained for Vectra-A and Vectra-C compare reasonably well with the reported PALS results for the HBA/HNA TLCPs.[24,46] The τ_3 values of around 1.2 ns were determined for the 75/25 HBA/HNA and 58/42 HBA/HNA TLCPs, while a τ_3 value for the 30/70 HBA/HNA TLCP was found to be lower.[46] A higher τ_3, 1.43 ns, was measured for a similar HBA/HNA TLCP (Vectra A900).[24] The τ_3 value of HX2000, 1.66 ns, agree well with the reported value, 1.685 ns, of a similar material, HX4000.[24] PC has the longest τ_3 of all materials used in this study, and its τ_3

Table III Free Volume Parameters by PALS and Densities for Various TLCPs and PC

Materials	τ_3 (ns)	I_3 (%)	V_f (Å^3)	h_f/C (% Å^3)	Density (g/cm^3)
Vectra-A	1.29 ± 0.03	10.28 ± 0.49	37.97 ± 2.14	390 ± 41	1.397 ± 0.002
Vectra-C	1.24 ± 0.06	5.38 ± 0.44	34.47 ± 4.07	183 ± 33	1.357 ± 0.003
Vectra-B	1.19 ± 0.42	0.69 ± 0.57	31.01 ± 26.89	22 ± 39	1.375 ± 0.002
HIQ45	1.39 ± 0.02	9.6 ± 0.31	45.82 ± 1.8	439 ± 28	1.395 ± 0.003
HX2000	1.66 ± 0.02	12.88 ± 0.22	67.07 ± 7.3	861 ± 100	1.263 ± 0.002
LC3000	1.29 ± 0.28	1.14 ± 0.37	37.97 ± 19.98	43 ± 37	1.394 ± 0.002
LC5000	1.18 ± 0.37	0.75 ± 0.31	30.42 ± 23.48	23 ± 27	1.396 ± 0.002
PC	2.03 ± 0.02	31.83 ± 0.36	99.52 ± 1.7	3167 ± 139	1.199 ± 0.003

compares well with values of various polycarbonate materials reported in other studies.[25,28,47]

As the free volume V_f represents the dimension of the free volume sites more explicitly than τ_3, the discussion of free volume sizes of various polymers will be given in terms of V_f. Volume of average free volume site V_f calculated by Eq.(4) and Eq. (5) from τ_3 values of various polymers presented here show the following order:

$$\text{PC} > \text{HX2000} > \text{HIQ45} > \text{Vectra-A} \cong \text{LC3000} > \text{Vectra-C} > \text{Vectra-B} > \text{LC5000}$$

The majority of TLCPs possess free volume sites about one-third the size of the free volume sites of PC. HX2000 possesses the largest free volume site among TLCPs, which is only two-third the size of PC. The significant interference of the phenyl substituents of HX2000 on molecular packing apparently is the dominant cause for it possessing the largest free volume magnitude found in TLCPs studied, although still smaller than PC. The smallest free volume demonstrated by LC5000 probably results from its greatest concentration of rigid HBA moiety, which encourages the very close molecular packing and thus frustrates the formation of larger free volume sites. In addition, the rather high degree of crystallinity, evidenced by its high value of ΔH_f (Table I), may also play a minor role since *o*-Ps predominantly probes the amorphous region. It is not yet clear to what extent the packing of chains in the crystalline regions differs from that of solid LC regions with the literature claiming that they are very similar in terms of density.[48] With a higher PET content, LC3000 has larger free volume sites than LC5000. A PET/50PHB TLCP (with 50 mol % HBA) has been found to have V_f of 50 Å^3,[49] greater than LC3000 whose HBA content is 60 mol %. The τ_3 of pure PET has been found to be around 1.8 ns, corresponding to a free volume site of 80 Å^3.[47] The incorporation of HBA into PET effectively changes its free volume size. With increasing HBA content, the sizes of free volume sites decrease from 80 Å^3 for pure PET to 30 Å^3 for LC5000 (80 mol % HBA).

Although Vectra-B contains a great amount of HNA unit (60 mol %) that frustrates *para* linearity of HBA unit, its free volume size is smaller than both Vectra-A (27 mol % HNA) and Vectra-C (15 mol % HNA). The reason for Vectra-B having such small value of τ_3 (and thus the small size of free volume sites) is likely due to its highly polar amide linkages. The presence of amide groups in polymers may lead to decreasing free volume size for a number of reasons. They can affect the molecular chain packing and thus free volume behavior by drawing the Vectra-B molecules close together via the formation of hydrogen bonds. In addition, they may also chemically influence the formation and annihilation of *o*-Ps as some electron acceptors such as nitrobenzene derivatives have been known to be capable of inhibiting as well as quenching *o*-Ps.[50] Quenching would lead to a decrease in τ_3, while inhibition would reduce the value of I_3. Therefore, when interpreting PALS results obtained from polymers with moieties that can chemically affect formation or lifetime of positron species, the possibility of quenching and inhibition has to be taken into account. The slightly smaller free volume of Vectra-C compared with that of Vectra-A might be due to its higher concentration of HBA, as the case of Rodrun TLCPs where LC5000 shows the smaller free volume site than LC3000. HIQ45 possesses the third largest free volume due to its frozen-in, biphasic structure[30] in which the isotropic phase is expected to have free volume sites potentially much larger than the anisotropic phase.

I_3 is a measure of the probability of *o*-Ps formation and is usually taken as indication of the number concentration of free volume sites in polymers if there is no moiety which will significantly inhibit the formation of *o*-Ps. In Table III, polymers whose τ_3 values are high in general also have higher mean I_3 values. Compared with PC, all TLCPs have lower concentrations of free volume sites. This is the result of both LC packing, as well as the partial crystallinity of the TLCPs (other than the amorphous HX2000) since it is thought that the *o*-Ps primarily forms and annihilates in the amorphous region.

In order to isolate the influence of molecular packing on I_3, the only amorphous TLCP, HX2000, in this study should be compared with PC. As stated previously, HX2000 has the highest I_3 value among all TLCPs due to its loose packing and lack of crystallinity. By contrast, PC contains more than twice the amount of free volume sites than HX2000. Although the bulky substituents of HX2000 are expected to promote the creation of free volume sites, the LC packing of HX2000 clearly still dominates in the sense that both size and number of free volume sites are less than the flexible PC. Surprisingly, Vectra-A has the second

highest I_3 in TLCPs and the reason is not fully understood. Vectra-C has a lower I_3 than Vectra-A since it comprises more *para* HBA units, which leads to a more linear structure. The PALS study of similar HBA/HNA materials has been reported to show I_3 values at about the same order of magnitude.[24,46] The very low value of I_3 shown by Vectra-B mainly results from chemical effects, that is, the presence of the amide groups which can inhibit the formation of *o*-Ps.[51] Although HIQ45 is likely to have the highest crystallinity as seen from its highest ΔH_f amongst all TLCPs, it possesses a high value of I_3 due to the contribution of its isotropic phase. Both LC3000 and LC5000 have very small I_3 values, 1.14 and 0.74%, respectively. The I_3 value reported for a PET/50PHB TLCP is of the order of a few percent,[50] which is slightly higher than the values found here but nevertheless very small. This may arise from a greater proportion of PET-rich phase where more free volume sites are present. PET shows I_3 ranging from 12 to 9% with crystallinity varying from 0 to 53%. The incorporation of HBA units in PET decreases I_3 from around 10% for neat PET to 1.14% for LC3000 (60% HBA) and 0.74% for LC5000 (80% HBA).

Note that PALS parameters for a given material determined in various research laboratories are not necessarily the same or even close. In addition to the intrinsic molecular packing, the instrument characteristics such as isotope used and software employed are all influential in the PALS results. Therefore, as a paper using PALS to study a number of TLCPs, the present work serves the purpose to differentiate PALS free volume properties of TLCPs using the same PALS apparatus, compared to reviewing PALS data as done by others.

Due to the unavailability of the C constant to calculate the free volume fraction by Eq. (6), a parameter, h_f/C, is used to evaluate and compare the free volume fraction of polymers. The values of h_f/C, as listed in Table III, take into account both the size and concentration of the free volume sites. The order of h_f/C of the polymers from large to small is

$$\text{PC} > \text{HX2000} > \text{HIQ45} > \text{Vectra-A} > \text{Vectra-C} > \text{LC3000} > \text{LC5000} > (\text{Vectra-B})$$

As a result of the combination of the largest free volume sites and highest concentration of free volume, PC has the greatest free volume fraction in this study. The bulky substituents of HX2000 hinder the crystallization process and also lead to less perfect molecular packing. Therefore, HX2000 has the highest free volume fraction among TLCPs. However, it still contains only about a quarter of the free volume present in PC due to its LC packing. HIQ45 has the third greatest level of h_f/C due to its isotropic regions, and possibly also the fact that it is a terpolymer and thus less likely to pack as well as Vectra TLCPs. Vectra-A with 73% HBA, compared with Vectra-C with about 85% HBA, appears to have a greater fraction of free volume. A higher HBA content in Vectra-C clearly improves the chain packing and reduces the presence of free volume sites as the smaller h_f/C of Vectra-C is predominantly contributed by reduced I_3. The h_f/C data for LC3000 and LC5000 is low due to the very low values of I_3, while the lowest h_f/C of Vectra-B is clearly the result of chemical effects of the amide groups rather than molecular packing.

As free volume is the origin of the glass transition phenomena of polymeric materials, it is tempting to see whether the free volume parameters derived from the PALS correlate well with the glass transition parameters such as T_g and tanδ. A plot of PALS parameters vs T_gs of polymers (except for Vectra-B whose PALS results are likely dominant by chemical influences on *o*-Ps formation) is shown in Figure 7. All PALS parameters indicate the trend that increases in size, number density and fraction of free volume sites of polymers lead to a higher T_g. This trend may seem to be contradictory to the idea that larger, greater number of free volume sites would facilitate the occurrence of glass transition and thus decrease T_g. For example, experimentally annealing a TLCP, HIQ40, has been shown to increase T_g with annealing time as well as annealing temperature due to improvement in molecular packing.[3] However, packing is in itself only part of picture. The ease of molecular mobility due to the molecular structure will also play an important role. Higher T_gs in LC materials can be achieved by incorporating kinked units such as meta linkages in HIQ45 and units which are difficult to rotate such as bulky substituents in HX2000.[42] Therefore, TLCPs which have greater T_gs due to reduction in ease of molecular mobility may intrinsically pack poorly and thus show greater free volume properties.

Figure 8 depicts the magnitude of tanδ at the glass transition correlating with the values of V_f,

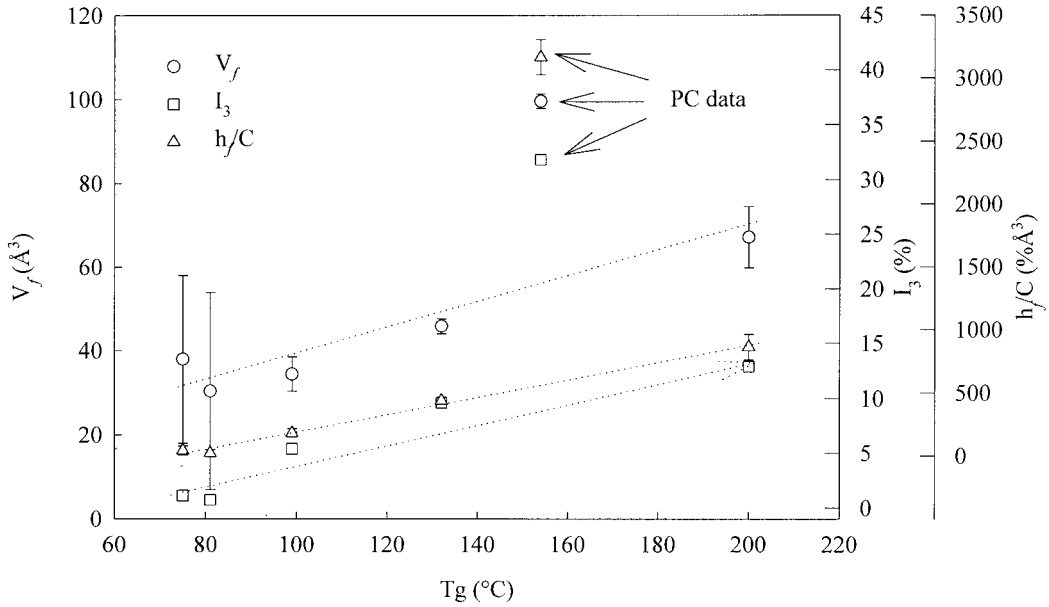

Figure 7 Correlation between T_g and PALS free volume parameters (T_g from DMA-7 data of Table II and PALS data from Table III).

I_3, and h_f/C. Although there are some fluctuations at the region of low tanδ, it is clear that greater values of V_f, I_3, and h_f/C correspond to stronger damping intensities. It is arguable as to whether the correlations between glass transition parameters and PALS parameters are valid, since PALS is performed at room temperature and the glass transition occurs at the higher temperature. It is possible that the free volume detected by PALS at low temperatures is responsible for the damping behavior at the glass transition. Since free volume is roughly frozen in below T_g, such an assumption is reasonable. As stated previously for Figure 8, TLCPs containing units that are capa-

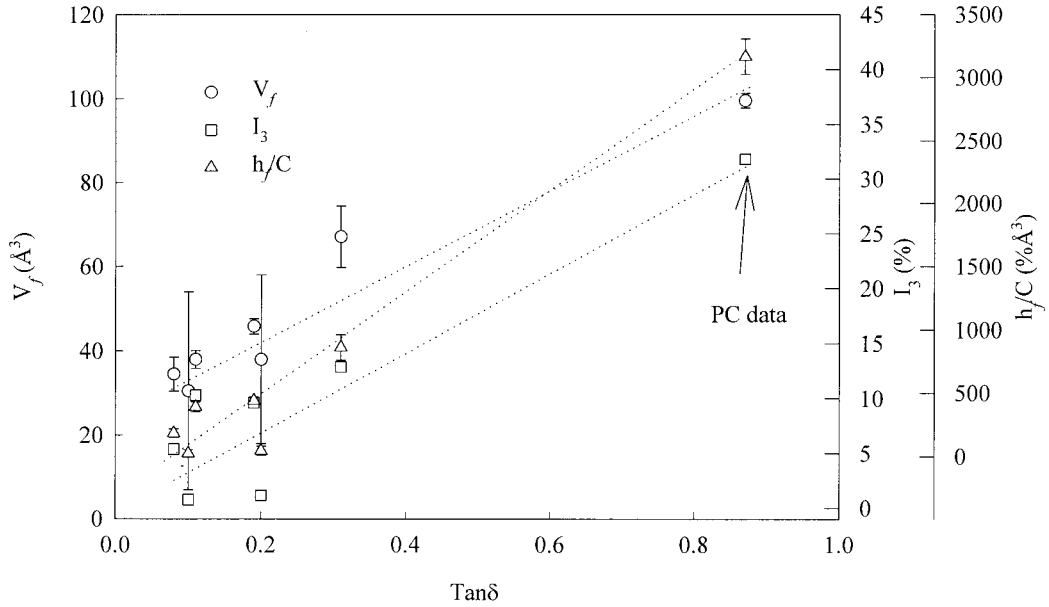

Figure 8 Correlation between damping strength and PALS free volume parameters (damping strength from DMA-7 data of Table II and PALS data from Table III).

ble of increasing T_g may also pack poorly. It follows that the greater free volume behavior measured by PALS, the greater chain mobility at T_g, and thus the higher value of tanδ.

PALS parameters have been used to interpret the changes of molecular packing of conventional thermoplastics from annealing,[9] and the mechanical performance resulting from such changes.[52] It could be problematic to attempt to correlate the free volume behavior determined under the undisturbed steady state with properties measured when the polymer undergoes changes in molecular alignment or even deformation. Another property that should be easier to correlate with PALS data is density. As the free volume is essentially the unoccupied space inside of the polymer, the bulk density of the polymer may well reflect its free volume fraction. A highly crystalline polymer should have a greater density compared with its amorphous analogue. If the polymer can also show LC order, it is logical to presume that the TLCPs would possess intermediate values of density according to the degree of molecular order. Table III also lists density values of the materials studied. The comparison between PC and TLCPs appears to be relatively straightforward with the TLCPs all having densities greater than 1.3 (except for HX2000 whose value is just below), as well as lower free volume fractions. Likewise, PC with a much larger free volume fraction shows a much lower density. Within the TLCPs, there are some anomalies. For example, Vectra-A with a seemingly less close-packed structure according to PALS has a very high density. In addition to free volume, density is also influenced by other factors. The most obvious one is, of course, crystallinity. However, the degree of crystallinity in TLCPs is thought to be low and it has been found that there is little difference in density of TLCP crystals and solid LC region.[53,54]

Figure 9 examines the correlation between h_f/C and density of polymers. In general, the macroscopic property, density, reflects what would be expected from the results of microscopic measurements, h_f/C of PALS. That is, a higher density corresponds to a lower h_f/C. However, it appears that other factors also affect density once the polymers are close packed as are TLCPs since the correlation is less obvious in the low h_f/C region. It is clear that other than the nanosized free volume space characterized by PALS, factors such as chain volume, chain conformation, and perhaps packing on larger size scales become important when free volume fraction is small.

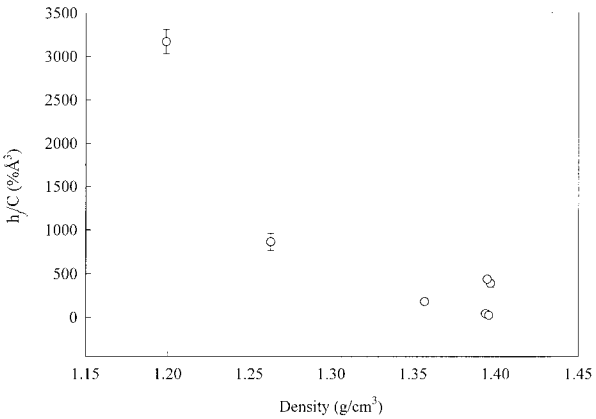

Figure 9 Correlation between density and free volume fraction index.

CONCLUSIONS

A wide selection of TLCPs was investigated with focus on their transition behavior and free volume properties. The melt and solid state properties of TLCPs are quite different from those of flexible polymers due to variation in the molecular packing. TLCPs exhibit distinct molecular alignment as a result of their rigid molecules, while conventional flexible polymers display entanglement networks. Molecular mobility of TLCPs possible during the glass transition is likely only to a lesser extent compared with that of flexible polymers such as PC. This is seen from their ill-defined glass transition behavior in the DSC thermograms and the rather low intensities of tanδ peaks by DMTA. It is found that TLCPs that more closely resemble flexible polymers with regards chain conformation exhibit more prominent glass transition behavior. This includes TLCPs, which contain more flexible segments (LC3000, LC5000), meta- linkages (HIQ45), or phenyl substituents along the main chains (HX2000). Heats of fusion (ΔH_f) of TLCPs are much lower than crystalline flexible polymers in the literature because the molecular order of TLCPs only changes from a crystalline state (or only a paracrystalline state[55]) to a liquid crystalline state rather than to an isotropic state as in conventional crystalline flexible polymers. Larger values of ΔH_f were found in TLCPs with hydrogen bonding (Vectra-B) or containing nonliquid crystalline phases (HIQ45).

Free volume on an angstrom scale exists in polymers due to imperfect packing of the long polymer chains. Positron annihilation lifetime spectroscopy, which is capable of detecting defect

structures in materials, was used to determine and allow comparison of free volume properties in polymers. The relatively extended molecular conformations of TLCPs due to their chain rigidity would be expected to result in free volume behavior quite different from that of flexible polymers. TLCPs are shown in this work to have relatively smaller, fewer free volume cavities than a linear thermoplastic such as PC. TLCPs with kinked moieties or bulky pendent substituents possess more, larger free volume. TLCPs containing amide groups show very small PALS parameters as *o*-Ps were chemically quenched and/or inhibited. PALS parameters of TLCPs and PC show correlations with their glass transition temperatures, damping intensities (peak heights of tanδ peaks by DMTA) and densities. This indicates that angstrom-sized free volume cavities probed by PALS in the glassy state are also important in determining molecular motions related to the glass transition. The seemingly contradictory T_g dependence of PALS parameter where higher T_g corresponds to larger, more free volume sites may result from molecular architecture of TLCPs. Some units in TLCPs such as meta linkages and pendent phenyl groups lead to higher T_gs due to difficulty in molecular rotation, even though it may give rise to poor packing of TLCPs. Density was found to correlate to the magnitude of the free volume fraction characterized by PALS. However, its dependence on chain volume, chain conformation and possibly packing on size scales larger than those probed by PALS becomes important when polymer chains are close packed.

We would like to thank the provision of a scholarship from the Targeted Institution Link (TIL) program of DEETYA (Australian Government) for TTH to study in Monash University, Australia. A Postgraduate Publication Award granted to TTH by Monash University for the preparation of this paper is also acknowledged.

REFERENCES

1. Wissbrun, K .F. Br Polym J 1980, December, 163.
2. Joseph, E.; Wilkes, G. L.; Baird, D. G. Polymer 1985, 26, 689.
3. Cantrell, G. R.; McDowell, C. C.; Freeman, B. D.; Noel, C. J. Polym Sci Polym Phys Ed 1999, 37, 505.
4. Troughton, M. J.; Davies, G. R.; Ward, I. M. Polymer 1989, 30, 58.
5. Ward, I. M. Makromol Chem Macromol Symp 1993, 69, 75.
6. Magagnini, P. In Thermotropic Liquid Crystalline Polymer Blends; La Mantia, F. P., Ed.; Technomic Publishing: Lancaster, 1993; Chap 1.
7. Jean, Y. C. In Positron Spectroscopy of Solid—Proceedings of the International School of Physics Enrico Fermi; Dupasquier, A., Mills, A. P., Eds., IOS Press: Amsterdam, 1995.
8. Simon, G. P. Trends Polym Sci 1997, 5, 394.
9. Bigg, D. M. Polym Sci Eng 1996, 36, 737.
10. Nakanishi, H.; Wang, S. J.; Jean, Y. C. In International Symposium on Positron Annihilation Studies of Fluids; Sharma, S. C., Ed.; World Scientific: Singapore, 1987.
11. Wang, Y. Y.; Nakanishi, H.; Jean, Y. C.; Sandreczki, T. C. J Polym Sci Polym Phys Ed 1990, 28, 1431.
12. Liu, J.; Deng, Q.; Jean, Y. C. Macromolecules 1993, 26, 7149.
13. Ramachandra, P.; Ramani, R.; Ramgopal, G.; Ranganathaiah, C. Eur Polym J 1997, 33, 1707.
14. Davies, W. J.; Pthrick, R. A. Eur Polym J 1994, 30, 1289.
15. Brandt, W.; Berko, S.; Walker, W. W. Phys. Rev., 120, 1289 (1960).
16. Kobayashi, Y.; Haraya, K.; Kamiya, Y.; Hattori, S. Bull Chem Soc Jpn 1992, 65, 160.
17. Schmidt, M.; Maurer, F. H. J. J Polym Sci Polym Phys Ed 1998, 36, 1061.
18. Schmidt, M.; Maurer, F. H. J. Proc World Polymer Congress—37th International Symposium on Macromolecules, Gold Coast, Australia, July 1998, 590.
19. Jean, Y. C.; Sandreczki, T. C.; Ames, D. P. J. Polym Sci Polym Chem Ed 1986, 24, 1247.
20. Deng, Q.; Sundar, C. S.; Jean, Y. C. J Phys Chem 1992, 96, 492.
21. Nakanishi, H.; Jean, Y. C.; Smith, E. G.; Sandreczki, T. C. J Polym Sci Polym Phys Ed 1989, 27, 1419.
22. Calundann, G. W.; Jaffe, M. Proc. Robert A. Welch Foundation Conference on Chemical Research. XXVI Synthetic Polymers, Houston, TX, 1982, p 247.
23. Wissbrun, K. F.; Kiss, G.; Cogswell, F. N. Chem Eng Comm 1987, 53, 149.
24. Naslund, R. A.; Jones, P. L. In MRS Symposium Proceedings—Submicron Multiphase Materials; Baney, R. H., Gilliom, L. R., Hirano, S. I., Schmidt, H. K., Eds.; Materials Research Society: Pittsburgh, PA, 1992; Vol 274, p 53.
25. Turek, D. E. Ph.D. thesis, Department of Materials Engineering, Monash University, Australia, 1992.
26. Jackson, W. J.; Kuhfuss, H. F. J Polym Sci Polym Chem Ed 1976, 14, 1043.
27. Izu, P.; Munoz, M. E.; Pena, J. J.; Santamaria, A. Polymer 1994, 35, 2422.
28. Campbell, J. A. Ph.D. thesis, Department of Materials Engineering, Monash University, Australia, 1998.

29. Cameron, G. G.; Chisholm, M. S. Polymer 1986, 27, 437.
30. Kiss, G. J Rheol 1986, 30, 585.
31. Gupta, B.; Calundann, G.; Charbonneau, L. F.; Linstid, H. C.; Shepherd, J. P.; Sawyer, L. C. J Appl Polym Sci 1994, 53, 575.
32. Baird, D. G.; Bafna, S. S.; De Souza, J. P.; Sun, T. Polym Compos 1993, 14, 214.
33. Bhattarcharya, S. K.; Tendolkar, A.; Misra, A. Mol Cryst Liq Cryst 1987, 153, 501.
34. Zachariades, A. E.; Economy, J.; Logan, J. A. J Appl Polym Sci 1982, 27, 719.
35. Economy, J.; Volksen, W.; Viney, C.; Geiss, R.; Siemens, R.; Karis, T. Macromolecules 21, 2777.
36. Jung, S. H.; Kim, S. C. Polym J 1988, 20, 73.
37. Green, D. I.; Davies, G. R.; Ward, I. M.; Alhaj-Mohammed, M. H.; Jawsd, S. A. Polym Adv Technol 1990, 1, 41.
38. McCullagh, C. M.; Blackwell, J. In Comprehensive Polymer Science—Second Supplement; Allen, G., Aggarwal, S. L., Russo, S., Eds., Pergamon: London, 1996.
39. Blundell, D. J.; Buckingham, K. A. Polymer 1985, 26, 1623.
40. Wissbrun, K. F.; Yoon, H. N. Polymer 1989, 30, 2193.
41. Simon, G. P.; Hsieh, T.-T. Unpublished work.
42. Donald, A. M.; Windle, A. H. Liquid Crystalline Polymers; Cambridge University Press: New York, 1992; Chap 3.
43. Nobile, M. R.; Amendola, E.; Nicolais, L.; Carfagna, C. Polym Eng Sci 1989, 29, 244.
44. Simon, G. P. In Mechanical and Thermophysical Properties of Polymer Liquid Crystals; Brostow, W., Ed.; Chapman and Hall: London, 1998.
45. Tokita, M.; Osada, K.; Watanabe, J. Polym J 1998, 30, 589.
46. McCullagh, C. M.; Blackwell, J.; Jamieson, A. M. Macromolecules 1995, 27, 2996.
47. Xie, L.; Gidley, D. W.; Hristov, H. A.; Yee, A. F. Polymer 1994, 35, 14.
48. Buijs, J. H. H. M.; Vroege, G. J. Polymer 1993, 34, 4692.
49. Uedono, A.; Sadamoto, R.; Kawano, T.; Tanigawa, S.; Uryu, T. J Polym Sci Polym Phys Ed 1995, 33, 891.
50. Hirata, K.; Kobayashi, Y.; Ujihira, Y. J Chem Soc Faraday Trans 1996, 92, 985.
51. Wästlund, C.; Maurer, F. H. J. Polymer 1998, 39, 2897.
52. Zipper, M. D.; Simon, G. P.; Tant, M. R.; Small, G. D.; Stack, G. M.; Hill, A. J. Polym Int 1995, 36, 127.
53. Hsiao, B. S.; Stein, R. S.; Deutscher, K.; Winter, H. H. J Polym Sci Polym Phys Ed 1990, 28, 1571.
54. Walsh, D. J.; Dee, G. T.; Wojtkowski, P. W. Polymer 1989, 30, 1467.
55. Hanna, S.; Windle, A. H. Polymer 1988, 29, 207.